Inorg. Chem. **2003**, *42*, 398–408

Nature of Copper(II)–Lanthanide(III) Magnetic Interactions and Generation of a Large Magnetic Moment with Magnetic Anisotropy of 3d–4f Cyclic Cylindrical Tetranuclear Complexes $[Cu^{II}LLn^{III}(hfac)_2]_2$, ($H_3L$ = 1-(2-Hydroxybenzamido)-2-(2-hydroxy-3-methoxybenzylideneamino)ethane and Hhfac = Hexafluoroacetylacetone, Ln^{III} = Eu, Gd, Tb, Dy)

Takafumi Kido, Yuichi Ikuta, Yukinari Sunatsuki, Yoshihiro Ogawa, and Naohide Matsumoto*

Department of Chemistry, Faculty of Science, Kumamoto University, Kurokami 2-39-1, Kumamoto 860-8555, Japan

Nazzareno Re

Facolta di Farmacia, Università degli Studi "G. D'Annunzio", I-66100 Chieti, Italy

Received September 19, 2002

A cyclic cylindrical 3d–4f tetranuclear structure, in which the 3d and 4f magnetic ions are arrayed alternately, has been found to be a suitable molecular design to produce a large magnetic moment and large magnetic anisotropy. Complexes **3**–**10** with the chemical formula $[MLLn(hfac)_2]_2$ ((M^{II}, Ln^{III}) = (Cu, Eu) (**3**), (Cu, Gd) (**4**), (Cu, Tb) (**5**), (Cu, Dy) (**6**), (Ni, Eu) (**7**), (Ni, Gd) (**8**), (Ni, Tb) (**9**), (Ni, Dy) (**10**)) have been synthesized, where H_3L = 1-(2-hydroxybenzamido)-2-(2-hydroxy-3-methoxybenzylideneamino)ethane and Hhfac = hexafluoroacetylacetone. The powder X-ray diffractions and FAB-mass spectra demonstrated that these complexes assume a similar tetranuclear structure. The crystal structures of **4** and **5** showed that each complex has a cyclic cylindrical tetranuclear $Cu^{II}_2Ln^{III}_2$ structure, in which the Cu^{II} complex functions as a "bridging ligand-complex" to two adjacent Ln^{III} ions. The temperature-dependent magnetic susceptibilities from 2 to 300 K and the field-dependent magnetizations at 2 K from 0 to 5 T have been measured for four pairs of $Cu^{II}_2Ln^{III}_2$ and $Ni^{II}_2Ln^{III}_2$, in which compound $Ni^{II}_2Ln^{III}_2$ containing diamagnetic Ni^{II} ion was used as the reference complex to evaluate the Cu^{II}–Ln^{III} magnetic interaction. Comparison of the magnetic properties of the $Cu^{II}_2Ln^{III}_2$ complex with those of the corresponding $Ni^{II}_2Ln^{III}_2$ complex showed that the magnetic interaction between Cu^{II} and Eu^{III} ions is weakly ferromagnetic and that between Cu^{II} and either of Gd^{III}, Tb^{III}, and Dy^{III} ions is ferromagnetic. Complex $Cu^{II}_2Gd^{III}_2$, **4**, has an $S = 8$ spin ground state, due to the ferromagnetic spin coupling between $S_{Gd} = {}^7/_2$ and $S_{Cu} = {}^1/_2$ with coupling constants of $J_1 = +3.1$ cm^{-1} and $J_2 = +1.2$ cm^{-1}. The magnetic measurements showed that compounds **5** and **6**, $Cu^{II}_2Ln^{III}_2$ (Ln^{III} = Tb, Dy), exhibit large magnetic moments and large magnetic anisotropy due to the Ln^{III} ion.

Introduction

The field of molecular-based magnetic materials has shown spectacular advances in the last two decades, especially for metal-complex-based magnetic compounds.[1] Assembly metal complexes exhibiting versatile magnetic behaviors[2] such as light switchable magnets[3] and single molecule magnets[4] have attracted special attention in the latest decade. The molecular-based magnetic materials consisting of d-transition metal ions have been well developed, and the magnetochemistry of d−f transition metal complexes will be one of the future targets

* To whom correspondence should be addressed. E-mail: naohide@aster.sci.kumamoto-u.ac.jp. Fax: +81-96-342-3390.

(1) Kahn, O. *Molecular Magnetism*; VCH: Weinheim, 1993.

(2) (a) Miller, J. S.; Calabrese, J. C.; Rommelmann, H.; Chittipeddi, S. R.; Zhang, J. H.; Reiff, W. M.; Epstein, A. J. *J. Am. Chem. Soc.* **1987**, *109*, 769−781. (b) Kahn, O.; Pei, Y.; Verdaguer, M.; Renard, J. P.; Sletten, J. *J. Am. Chem. Soc.* **1988**, *110*, 782−789. (c) Miyasaka, H.; Matsumoto, N.; Okawa, H.; Re, N.; Gallo, E.; Floriani, C. *J. Am. Chem. Soc.* **1996**, *118*, 981−994. (d) Tamaki, H.; Zhong, Z.; Matsumoto, N.; Kida, S.; Koikawa, M.; Achiwa, N.; Hashimoto, Y.; Okawa, H. *J. Am. Chem. Soc.* **1992**, *114*, 6974−6979. (e) Zhong, Z. J.; Seino, H.; Mizobe, Y.; Hidai, M.; Fujishima, A.; Ohkoshi, S.; Hashimoto, K. *J. Am. Chem. Soc.* **2000**, *122*, 2952−2953.

10.1021/ic026045d CCC: $25.00
Published on Web 12/17/2002

in this field. Since Gatteschi and co-workers discovered a ferromagnetic coupling between Cu^{II} and Gd^{III} ions in 1985,[5] several 3d−4f polynuclear complexes including dinuclear $Cu^{II}Gd^{III}$, trinuclear $Cu^{II}_2Gd^{III}$, tetranuclear $Cu^{II}_2Gd^{III}_2$, and other 3d−4f metal complexes have been reported.[6] However, the coexisting antiferromagnetic coupling within a Cu^{II}_2 pair often concealed the weak $Cu^{II}-Gd^{III}$ ferromagnetic coupling and resulted in net antiferromagnetic behavior. Thus, it is essential for further development of 3d−4f magnetochemistry to obtain accurate information on the 3d−4f magnetic interaction[7] and to find a synthetic design without 3d−3d and 4f−4f magnetic interactions. A cyclic cylindrical 3d−4f polynuclear structure, in which the 3d and 4f magnetic ions are arrayed alternately, can be one of the most suitable molecular designs not only to generate a molecule without 3d−3d and 4f−4f magnetic interactions but also to produce a large magnetic moment, because the 3d−3d and 4f−4f magnetic interactions are negligibly small due to nonbridging ligands between them and the magnetic arrangement of the adjacent 3d and 4f magnetic ions is simply assembled depending on the 3d−4f magnetic interaction. The effectiveness of this molecular design for this purpose has been examined by us[8] and Costes et al.[9] We have reported preliminary information about the cyclic tetranuclear $Cu^{II}_2Gd^{III}_2$ complex, **4**, which has an $S = 8$ spin ground state derived from the ferromagnetic spin coupling between Gd^{III} ion ($^8S_{7/2}$, $S_{Gd} = {}^7/_2$) and Cu^{II} ion ($S_{Cu} = {}^1/_2$).[8] If the magnetically isotropic Gd^{III} ion ($S = {}^7/_2$, $L = 0$, $J = {}^7/_2$, $^8S_{7/2}$) was substituted for the other magnetically anisotropic lanthanide(III) ion in this tetranuclear structure, a discrete 3d−4f tetranuclear molecule exhibiting a large magnetic moment and magnetic anisotropy can be obtained. Such a compound may be a good candidate as a novel single molecule magnet, because single molecule magnets have been found in the Mn and Fe cluster molecules with a large spin ground state and magnetic anisotropy.[10] To introduce magnetic anisotropy into the tetranuclear molecule, a series of Ln^{III} ions with $4f^{6-9}$ electronic configurations, Eu^{III}, Gd^{III}, Tb^{III}, and Dy^{III}, were used, because the electronic structure of the ground state is $^7F_0$ ($S = 3$, $L = 3$, $J = 0$) for Eu^{III}, $^8S_{7/2}$ ($S = {}^7/_2$, $L = 0$, $J = {}^7/_2$) for Gd^{III}, $^7F_6$ ($S = 3$, $L = 3$, $J = 6$) for Tb^{III}, and $^6H_{15/2}$ ($S = {}^5/_2$, $L = 5$, $J = {}^{15}/_2$) for Dy^{III}, respectively. These ions, with the sole exception of Gd^{III}, exhibit magnetic anisotropy due to the first-order orbital angular momentum. In this study, we synthesized a series of cyclic cylindrical tetranuclear 3d−4f complexes, $[MLLn(hfac)_2]_2$ (M^{II}, Ln^{III}) = (Cu, Eu) (**3**), (Cu, Gd) (**4**), (Cu, Tb) (**5**), (Cu, Dy) (**6**), (Ni, Eu) (**7**), (Ni, Gd) (**8**), (Ni, Tb) (**9**), and (Ni, Dy) (**10**) [H_3L = 1-(2-hydroxybenzamido)-2-(2-hydroxy-3-methoxybenzylideneamino)ethane and Hhfac = hexafluoroacetylacetone]. Here, we report their syntheses, structures, and magnetic properties.

Results and Discussion

Synthesis and Characterization of Cyclic Cylindrical Tetranuclear $Cu^{II}_2Ln^{III}_2$ and $Ni^{II}_2Ln^{III}_2$ Complexes $[MLLn(hfac)_2]_2$ (M^{II} = Cu^{II}, Ni^{II}; Ln^{III} = Eu^{III}, Gd^{III}, Tb^{III}, Dy^{III}). For the purpose of the construction of such a cyclic cylindrical 3d−4f polynuclear structure, an assembly reaction between the Cu^{II} or Ni^{II} complex K[ML] as 3d-component and $Ln(hfac)_3(H_2O)_2$ as 4f-component was performed. The molecular structures of two components and the cyclic cylindrical 3d−4f tetranuclear complex constructed by the assembly reaction are shown in Scheme 1. The Cu^{II} or Ni^{II} complex with the tetradentate ligand of the 1:1:1 condensation product of 3-methoxysalicylaldehyde, ethylenediamine, and 2-hydroxybenzamide functions as a "bridging ligand-complex" to Ln^{III} component complex $Ln(hfac)_3(H_2O)_2$ that exhibits substitutable coordination sites. The phenoxo and methoxy oxygen atoms of the Cu^{II} or Ni^{II} component coordinate to one Ln^{III} ion, and further, the amide oxygen atom at the opposite side coordinates to another Ln^{III} ion to result in an alternate and cyclic array of the 3d−4f metal ions. As a counterpart, the Ln^{III} complex $Ln(hfac)_3(H_2O)_2$ was used, because the hexafluoroacetylacetonato ($hfac^-$) ion can be easily substituted with stronger external donor

(3) (a) Decurtins, S.; Gütlich, P.; Kohler, C. P.; Spiering, H.; Hauser, A. *Chem. Phys. Lett*. **1984**, *105*, 1. (b) Decurtins, S.; Gütlich, P.; Hasselbach, K. M.; Hauser, A.; Spiering, H. *Inorg. Chem.* **1985**, *24*, 2174−2178. (c) Gütlich, P.; Garcia, Y.; Woike, T. *Coord. Chem. Rev.* **2001**, *219*−*221*, 839−879. (d) Ohkoshi, S.; Hashimoto, K. *J. Am. Chem. Soc.* **1999**, *121*, 10591−10597. (c) Sato, O.; Iyoda, T.; Fujishima, A.; Hashimoto, K. *Science* **1996**, *272*, 704−705. (f) Hayami, S.; Gu, Z.; Shiro, M.; Einaga, A.; Fujishima, A.; Sato, O. *J. Am. Chem. Soc.* **2000**, *122*, 7126−7127.

(4) (a) Sessoli, R.; Gatteschi, D.; Caneschi, A.; Novak, M. A. *Nature* **1993**, *365*, 141−143. (b) Gatteschi, D.; Caneschi, A.; Pardi, L.; Sessoli, R. *Science* **1994**, *265*, 1054−1058. (c) Sessoli, R.; Tsai, H. L.; Schake, A. R.; Wang, S.; Vincent, J. B.; Folting, K.; Gatteschi, D.; Christou, G.; Hendrickson, D. N. *J. Am. Chem. Soc.* **1993**, *115*, 1804−1816. (d) Thomas, L.; Lionti, F.; Ballou, R.; Gatteschi, D.; Sessoli, R.; Barbara, B. *Nature* **1996**, *383*, 145−147. (e) Cadiou, C.; Murrie, M.; Paulsen, C.; Villar, V.; Wernsdorfer, W.; Winpenny, W. E. P. *Chem. Commun*. **2001**, 2666−2667. (f) Shores, M. P.; Sokol, J. J.; Long, J. R. *J. Am. Chem. Soc*. **2002**, *124*, 2279−2292. (g) Boskovic, C.; Brechin, E. K.; Streib, W. E.; Folting, K.; Bollinger, J. C.; Hendrickson, D. N.; Christou, G. *J. Am. Chem. Soc.* **2002**, *124*, 3725−3736.

(5) Bencini, A.; Benelli, C.; Caneschi, A.; Carlin, R. L.; Dei, A.; Gatteschi, D. *J. Am. Chem. Soc*. **1985**, *107*, 8128−8136.

(6) (a) Benelli, C.; Caneschi, A.; Gatteschi, D.; Guillou, O.; Pardi, L. *Inorg. Chem.* **1990**, *29*, 1750−1755. (b) Benelli, C.; Fabretti, A. C.; Giusti, A. *J. Chem. Soc., Dalton Trans.* **1993**, 409−412. (c) Bencini, A.; Benelli, C.; Caneschi, A.; Dei, A.; Gatteschi, D. *Inorg. Chem.* **1986**, *25*, 572−575. (d) Kahn, M. L.; Mathoniere, C.; Kahn, O. *Inorg. Chem.* **1999**, *38*, 3692−3697. (e) Benelli, C.; Murrier, M.; Parsons, S.; Winpenny, R. E. P. *J. Chem. Soc., Dalton Trans.* **1999**, 4125−4126. (f) Winpenny, R. E. P. *Chem. Soc. Rev.* **1998**, *27*, 447. (g) Guillou, O.; Bergerat, P.; Kahn, O.; Bakalbassis, E.; Boubekeur, K.; Batail P.; Guillot, M. *Inorg. Chem.* **1992**, *31*, 110−114. (h) Benelli, C.; Murie, M.; Parsons, S.; Winpenny, R. E. *J. Chem. Soc., Dalton Trans.* **1999**, 4125−4126. (i) Figuerola, A.; Diaz, C.; Fallash, M. S. E.; Ribas, J.; Maestro, M.; Mahfa, J. *Chem. Commun.* **2001**, 1204−1205. (j) Liang, Y.; Cao, R.; Su, W.; Hong, M.; Zhang, W. *Angew. Chem., Int. Ed.* **2000**, *39*, 3304−3307. (k) Brewer, C.; Brewer, G.; Scheidt, W. R.; Shang, M.; Carpenter, E. E. *Inorg. Chim. Acta* **2001**, *313*, 65−70.

(7) (a) Costes, J.-P.; Dahan, F.; Dupuis, A.; Laurent, J.-P. *Inorg. Chem.* **2000**, *39*, 169−173. (b) Costes, J.-P.; Dahan, F.; Dupuis, A. *Inorg. Chem.* **2000**, *39*, 165−168. (c) Costes, J.-P.; Dahan, F.; Dupuis, A.; Laurent, J.-P. *Inorg. Chem.* **1997**, *36*, 3429−3433. (d) Sasaki, M.; Manseki, K.; Horiuchi, H.; Kumagai, M.; Sakamoto, M.; Sakiyama, H.; Nishida, Y.; Sakai, M.; Sadaoka, Y.; Ohba, M.; Okawa, J. *J. Chem. Soc., Dalton Trans.* **2000**, 259−263. (e) Chen, Q. Y.; Luo, Q. H.; Zheng, L. M.; Wang, Z. L.; Chen, J. T. *Inorg. Chem.* **2002**, *41*, 605−609.

(8) Kido, T.; Nagasato, S.; Sunatsuki, Y.; Matsumoto, N. *Chem. Commun.* **2000**, 2113-2114.

(9) Costes, J.-P.; Dahan, F. *C. R. Acad. Sci., Ser. IIc: Chim.* **2001**, *4*, 97−103.

(10) Gatteschi, D.; Sessoli, R.; Cornia, A. *Chem. Commun.* **2000**, 725−732.

Scheme 1

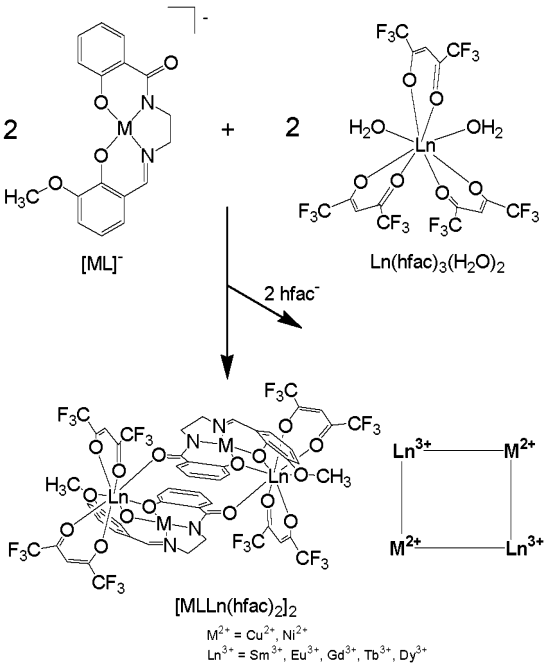

atoms and can also function as a mononegative capping or terminal ligand.

The simple mixing of methanolic solutions of K[ML] (M^{II} = Cu^{II}, Ni^{II}) and $Ln(hfac)_3(H_2O)_2$ (Ln^{III} = Eu^{III}, Gd^{III}, Tb^{III}, Dy^{III}) in a 1:1 mol ratio gave 3d−4f heterometal complexes with the chemical formula $[MLLn(hfac)_2]_2$, **3**−**10**, in high yields (83−91%), where one $hfac^-$ ligand per Ln^{III} ion is eliminated during the reaction to give an electrically neutral species, $[MLLn(hfac)_2]_2$. Each infrared spectrum exhibits an intense absorption band assignable to the $\nu_{C=O}$ vibration of the amido moiety at 1651−1652 cm^{-1}, whose wavenumber is shifted to a higher wavenumber value from 1644 cm^{-1} of the component complex K[CuL] and from 1625 cm^{-1} of K[NiL].[11] The shift is related to the weaker coordination of the amido group to the Ln^{III} ion, compared with the coordination of the amido group to the K^+ ion.[12] Because Cu^{II}−Ln^{III} complexes **3**−**6** are sparingly soluble in water and common organic solvents, recrystallization and physical measurements in the solution state were not performed. Compounds **7**−**10** are slightly soluble in *N*,*N*-dimethylformamide (DMF).

Structural Description of $[CuLGd(hfac)_2]_2$ (4) and $[CuLTb(hfac)_2]_2$ (5). The powder X-ray diffraction patterns showed that Cu^{II}−Ln^{III} complexes **3**−**6** are isomorphous to each other. The X-ray powder diffraction patterns demonstrated that Ni^{II}−Ln^{III} complexes **7**−**10** are isomorphous to each other but are not isomorphous to Cu^{II}−Ln^{III} complexes **3**−**6**. Each FAB-mass spectrum shows a molecular ion peak corresponding to the tetranuclear structure $[Ni_2L_2Ln_2(hfac)_3]^+$, indicating that Ni^{II}−Ln^{III} complexes assume a similar cyclic tetranuclear structure to Cu^{II}−Ln^{III} complexes.

(11) Nakamoto, K. In *Infrared and Raman Spectra of Inorganic and Coordination Compounds*, 5th ed.; John Wiley and Sons: New York, 1997; Part B, Chapter III-14.

(12) Sunatsuki, Y.; Matsuo, T.; Nakamura, M.; Kai, F.; Matsumoto, N.; Tuchagues, J.-P. *Bull. Chem. Soc. Jpn.* **1998**, *71*, 2611−2619.

Table 1. X-ray Crystallographic Data for $[CuLGd(hfac)_2]_2$ (**4**) and $[CuLTb(hfac)_2]_2$ (**5**)

	$[CuLGd(hfac)_2]_2$ (**4**)	$[CuLTb(hfac)_2]_2$ (**5**)
formula	$C_{27}H_{17}N_2O_8CuGd$	$C_{27}H_{17}N_2O_8CuTb$
fw	946.22	947.89
space group	$P\bar{1}$ (No. 2)	$P\bar{1}$ (No. 2)
a, Å	11.055(5)	11.052(4)
b, Å	16.172(4)	16.144(6)
c, Å	10.284(3)	10.291(3)
α, deg	105.96(2)	106.20(4)
β, deg	114.61(2)	114.79(3)
γ, deg	80.47(3)	80.33(4)
V, Å^3	1604.4(1)	1598.0(1)
Z	2	2
D_{calcd}, g cm^{-3}	1.958	1.970
μ, cm^{-1}	28.37	29.76
R, R_w	0.036, 0.056	0.041, 0.052

Table 2. Relevant Coordination Bond Distances (Å) for $[CuLGd(hfac)_2]_2$ (**4**) and $[CuLTb(hfac)_2]_2$ (**5**)

$[CuLGd(hfac)_2]_2$ (**4**)		$[CuLTb(hfac)_2]_2$ (**5**)	
Cu−Cu*[a]	4.953(2)	Cu−Cu*	4.934(3)
Gd−Gd*	7.886(3)	Tb−Tb*	7.852(5)
Cu−Gd	3.432(1)	Cu−Tb	3.411(2)
Cu−Gd*	5.620(3)	Cu−Tb*	5.600(3)
Cu−N(1)	1.912(4)	Cu−N(1)	1.912(4)
Cu−N(2)	1.936(4)	Cu−N(2)	1.927(5)
Cu−O(2)	1.906(3)	Cu−O(2)	1.905(4)
Cu−O(3)	1.953(3)	Cu−O(3)	1.941(3)
Gd*−O(1)	2.275(3)	Tb*−O(1)	2.241(4)
Gd−O(2)	2.467(3)	Tb−O(2)	2.445(3)
Gd−O(3)	2.350(3)	Tb−O(3)	2.338(4)
Gd−O(4)	2.542(3)	Tb−O(4)	2.535(4)
Gd−O(5)	2.405(4)	Tb−O(5)	2.388(4)
Gd−O(6)	2.377(4)	Tb−O(6)	2.363(4)
Gd−O(7)	2.337(4)	Tb−O(7)	2.316(4)
Gd−O(8)	2.407(4)	Tb−O(8)	2.381(4)

[a] The asterisk denotes the symmetry operation of $-x, -y, -z$.

The crystal structures of **4** and **5** were determined by single-crystal X-ray diffraction analyses. Their crystallographic data are summarized in Table 1, demonstrating that they are isomorphous to each other. Selected bond distances with their estimated standard deviations in parentheses are given in Table 2. As **4** is isomorphous to **5**, only the structure of **4** is described in detail. Figure 1 shows a cyclic $Cu^{II}_2Gd^{III}_2$ tetranuclear structure of **4** with the atom numbering scheme, in which the molecule has an inversion center and the Cu^{II} and Gd^{III} ions are arrayed alternately. The Cu^{II} ion has square planar coordination geometry with the N_2O_2 donor atoms of the nonequivalent tetradentate ligand L. The Cu−N and Cu−O distances of the 2-oxybenzamido moiety (Cu−N(1) = 1.912(4) Å, Cu−O(2) = 1.906(3) Å) are considerably shorter than the corresponding values of the 2-oxy-3-methoxybenzaldehyde moiety (Cu−N(2) = 1.936(4) Å, Cu−O(3) = 1.953(3) Å). In the cyclic structure, the Cu^{II} complex functions as an electrically mononegative "bridging ligand-complex" to the two Gd^{III} ions. The two phenoxo (O(2) and O(3)) and the methoxy (O(4)) atoms at one side of the planar Cu^{II} complex coordinate to a Gd^{III} ion as a tridentate ligand with distances of Gd−O(2) = 2.467(3) Å, Gd−O(3) = 2.350(3) Å, Gd−O(4) = 2.542(3) Å, and Cu···Gd = 3.432(1) Å. The amido oxygen atom (O(1)) on the opposite side of the Cu^{II} complex coordinates to another Gd^{III} ion as a monodentate ligand with the distance of Gd*−O(1) = 2.275(3) Å and Cu···Gd* = 5.620(3) Å. Including the

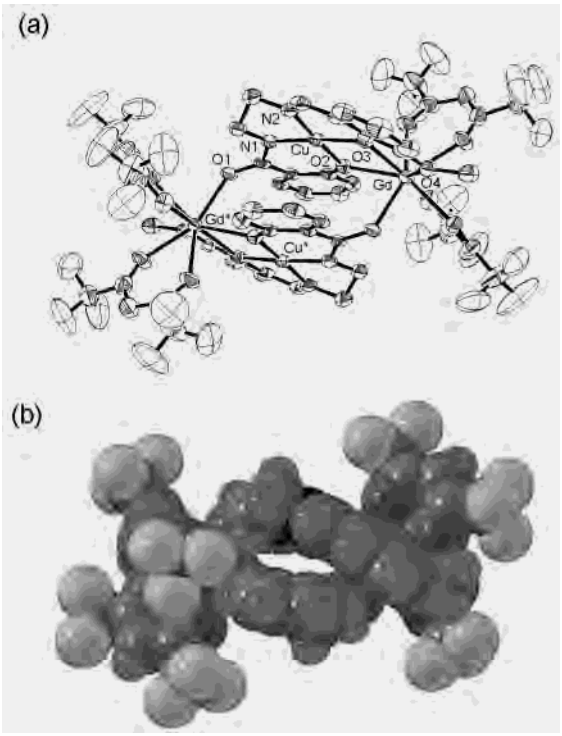

Figure 1. (a) Molecular structure of cyclic cylindrical tetranuclear complex $[CuLGd(hfac)_2]_2$ (**4**) with 30% thermal probability ellipsoids and selected atom labeling scheme. The hydrogen atoms are omitted for clarity. (b) Space filling representation of **4** showing cyclic cylindrical molecular structure with a hollow space.

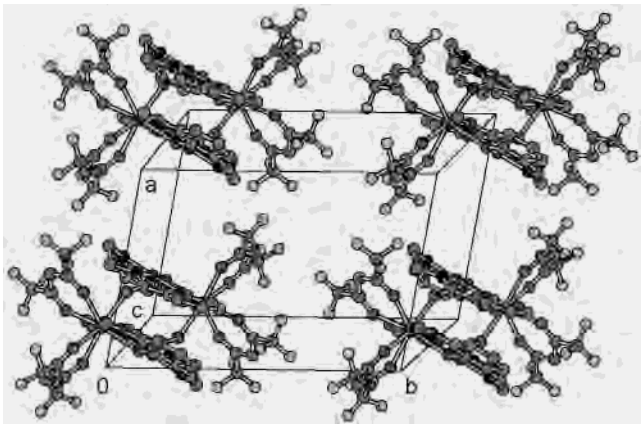

Figure 2. Packing diagram of the crystal structure **4**, showing that cyclic cylindrical tetranuclear molecules are well separated in the crystal lattice.

coordination of the two $hfac^-$ ions as a bidentate chelate ligand (Gd−O = 2.337(4)−2.407(4) Å), the Gd^{III} ion has an octacoordinate geometry with the O_8 oxygen atoms. It should be noted that the Gd−O bond distance with the amido oxygen is the shortest among the eight Gd−O bonds. In a cyclic structure, there is no bridging ligand between the two Cu^{II} ions and between the two Gd^{III} ions. The Cu···Cu* and Gd···Gd* distances are 4.953(2) and 7.886(3) Å, respectively, indicating that each metal ion pair is well separated. Figure 2 shows the packing diagram of **4** in the crystal, demonstrating that cyclic tetranuclear molecules are well separated in the crystal and the compound can be described as a magnetically isolated molecule.

Magnetic Properties. For many rare earth compounds, the $\chi_M T$ value at room temperature is close to what is predicted in the free-ion approximation for the case where only one level, $^{2S+1}L_J$, is thermally populated and second-order contributions are ignored.[1] The experimental magnetic susceptibilities of the present 3d−4f tetranuclear complexes can be compared with the calculated values derived from the equation $\chi_M = 2\chi_{3d} + 2\chi_{4f}$, in which χ_{3d} and χ_{4f} can be evaluated by eqs 1 and 2, respectively. On the other hand, for the complexes containing Eu^{III} ions, the magnetic susceptibility is affected by the thermally populated excited states because of the spin−orbit coupling, and more complicated expressions need to be used, see later.

$$\chi_{3d} = (Ng^2\beta^2/3kT)[S(S+1)] \quad (1)$$

$$\chi_{4f} = (Ng_J^2\beta^2/3kT)[J(J+1)],\ g_J = {}^3/_2 + [S(S+1) - L(L+1)]/2J(J+1) \quad (2)$$

The magnetic susceptibilities were measured under an external applied magnetic field of 1 T in the temperature range 2−300 K. The field-dependent magnetizations were measured at 2 K in the applied magnetic field range 0−5 T. The nature of the magnetic interaction between Cu^{II} and Ln^{III} ions was investigated by an empirical approach developed by Costes et al.[13] and Kahn et al.[14] on the basis of a comparison of the magnetic susceptibilities of $Cu^{II}_2Ln^{III}_2$ and isostructural $Ni^{II}_2Ln^{III}_2$ involving the diamagnetic Ni^{II} ion. In the approach of Costes et al. for the dinuclear 3d−4f complexes, the difference between the $\chi_M T$ values for isostructural Cu^{II}−Ln^{III} and Ni^{II}−Ln^{III} dimers, $\Delta(T)$, is obtained from eq 3, where $(\chi_M T)_{Cu}$ is the Curie constant and represents the $\chi_M T$ value attributable to an isolated Cu^{II} ion, while the temperature-dependent contribution $J_{CuLn}(T)$ is related to the nature of the overall exchange interactions between the Cu^{II} and Ln^{III} ions; in particular, a positive or a negative value of this contribution has been directly related to a ferro- or antiferromagnetic interaction, respectively.

$$\Delta(T) = (\chi_M T)_{CuLn} - (\chi_M T)_{NiLn} = (\chi_M T)_{Cu} + J_{CuLn}(T) \quad (3)$$

By assuming negligible intramolecular Ln^{III}−Ln^{III} and Cu^{II}−Cu^{II} magnetic interactions, see later, we have applied this approach to our cyclic tetranuclear $Cu^{II}_2Ln^{III}_2$ and isostructural $Ni^{II}_2Ln^{III}_2$ complexes for which we can immediately write eq 4.

$$\Delta(T) = (\chi_M T)_{Cu2Ln2} - (\chi_M T)_{Ni2Ln2} = 2(\chi_M T)_{Cu} + 2J_{CuLn}(T) \quad (4)$$

We tried to extend the Costes approach to the differences between the magnetization as a function of the applied magnetic field for $Cu^{II}_2Ln^{III}_2$ and isostructural $Ni^{II}_2Ln^{III}_2$ species. This difference may be obtained from eq 5, where $2M_{Cu}(H)$ is the magnetization for two independent Cu^{II} ions

(13) Costes, J.-P.; Dahan, F.; Dupuis, A.; Laurent, J.-P. *Chem. Eur. J.* **1998**, *4*, 1616−1620.
(14) Kahn, M. L.; Mathoniere, C.; Kahn, O. *Inorg. Chem.* **1999**, *38*, 3692−3697.

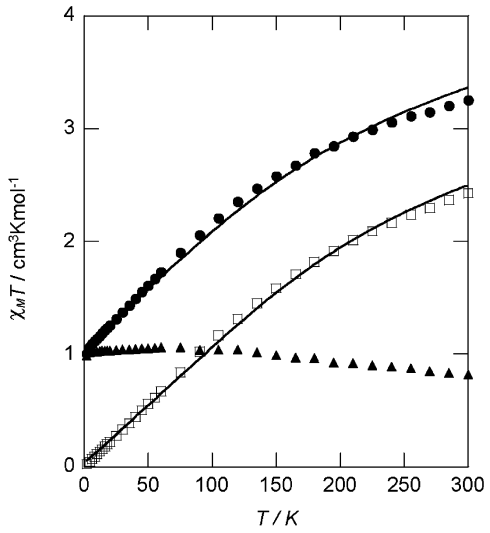

Figure 3. Plots of $\chi_M T$ vs temperature for $[CuLEu(hfac)_2]_2$ (**3**) (●) and $[NiLEu(hfac)_2]_2$ (**7**) (□), and for the difference $\Delta(T) = (\chi_M T)_{Cu2Eu2} - (\chi_M T)_{Ni2Eu2}$ (▲). The solid lines for **3** and **7** represent the theoretical curves derived from eq 6 with the parameter $\lambda = +397$ cm^{-1}.

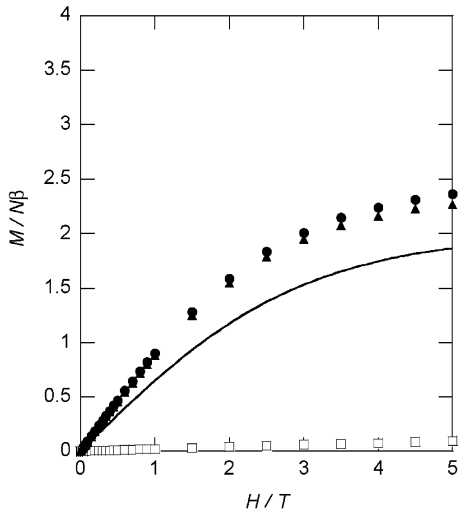

Figure 4. Field dependence of the magnetization of $[CuLEu(hfac)_2]_2$ (**3**) (●), $[NiLEu(hfac)_2]_2$ (**7**) (□), and the difference $\Delta(H) = M_{Cu2Eu2}(H) - M_{Ni2Eu2}(H)$ (▲) at 2 K. The solid line represents the theoretical curve for the sum of the Brillouin functions for two Cu^{II} ions with $S = {}^1/_2$ and $g = 2.00$.

and may be calculated by the Brillouin functions for two Cu^{II} ions with $S = {}^1/_2$ and $g = 2.00$, while the extra contribution $2J_{CuLn}(H)$ is related to the nature of the overall exchange interactions between the Cu^{II} and Ln^{III} ions.

$$\Delta(H) = M_{Cu2Ln2}(H) - M_{Ni2Ln2}(H) = 2M_{Cu}(H) + 2J_{CuLn}(H) \quad (5)$$

As the quantity $(\Delta(H) - 2M_{Cu}(H))$ represents the deviation from the limit situation for two Cu^{II} and two Ln^{III} ions that are magnetically independent, positive values of $J_{CuLn}(H)$, that is, $\Delta(H)$ lies above $2M_{Cu}(H)$, indicate ferromagnetic Cu^{II}−Ln^{III} interactions while negative values of $J_{CuLn}(H)$, that is, $\Delta(H)$ lies below $2M_{Cu}(H)$, indicate antiferromagnetic Cu^{II}−Ln^{III} interactions.

Magnetic Properties of $[CuLEu(hfac)_2]_2$ (3) and $[NiLEu(hfac)_2]_2$ (7). The magnetic behavior of **3** and **7** is shown in Figure 3, as plots of $\chi_M T$ versus T, where χ_M is the magnetic susceptibility per tetrameric molecule and T the absolute temperature. The $\chi_M T$ value of **7** is 2.42 cm^3 K mol^{-1} at 300 K, this value being inconsistent with the calculated value of 0.00 cm^3 K mol^{-1} expected for two diamagnetic Ni^{II} and two independent Eu^{III} ions, where the calculated values are derived from eqs1 and 2 and it is assumed that only the ground state $^7F_0$ of the Eu^{III} ion ($4f^6$, $J = 0$, $S = 3$, $L = 3$, $^7F_0$) is thermally populated. The disagreement is ascribed to the presence of thermally populated excited states, as is well-known for Eu^{III} complexes. On lowering the temperature, the $\chi_M T$ value decreases monotonically to zero. The temperature dependence of the magnetic susceptibility of **7** involving the diamagnetic Ni^{II} ion can be reproduced by expression 6, which takes into account the seven states $^7F_0$, $^7F_1$, $^7F_2$, $^7F_3$, $^7F_4$, $^7F_5$, and $^7F_6$ generated by the interelectronic repulsion and spin−orbit coupling.[15] The best-fit parameter $\lambda = +397$ cm^{-1} was obtained (with an agreement factor R of 1×10^{-3}), and the value is comparable with that reported for other Eu^{III} compounds with an analogous O_8 coordination.[15] The temperature dependence of magnetic susceptibility of **3** is reproduced by the equation $\chi_M = 2\chi_{Eu} + 2\chi_{Cu}$ with $\lambda = +397$ cm^{-1} and $\chi_{Cu} = Ng^2\beta^2/4kT$.

$$\chi_{Eu} = (N\beta^2/3kTx)[24 + (27x/2 - 3/2)e^{-x} + (135x/2 - 5/2)e^{-3x} + (189x - 7/2)e^{-6x} + (405x - 9/2)e^{-10x} + (1485x/2 - 11/2)e^{-15x} + (2457x/2 - 13/2)e^{-21x}]/[1 + 3e^{-x} + 5e^{-3x} + 7e^{-6x} + 9e^{-10x} + 11e^{-15x} + 13e^{-21x}], \text{ with } x = \lambda/kT \quad (6)$$

Comparison of the magnetic properties of **3** with those of **7** gives information on the intramolecular magnetic interaction between Cu^{II} and Eu^{III} ions. The difference $\Delta(T) = (\chi_M T)_{Cu2Eu2} - (\chi_M T)_{Ni2Eu2}$ is plotted in Figure 3. The $\Delta(T)$ value is in the range from 0.82 cm^3 K mol^{-1} at 300 K to 1.05 cm^3 K mol^{-1} below 75 K. Because $\Delta(T)$ is slightly larger than the contribution due to two noninteracting Cu^{II} ions, 0.75 cm^3 K mol^{-1}, $J_{CuEu}(T)$ can be estimated to be small positive or nearly zero, suggesting that there is no substantial magnetic interaction between Cu^{II} and Eu^{III} ions. This result is consistent with that reported by Costes for an analogous dinuclear Cu^{II}Eu^{III} complex.[13]

Figure 4 shows the field dependence of the magnetization up to 5 T at 2 K for **3** and **7**, as plots of the experimental values of $M/N\beta$ versus H. On increasing the applied external magnetic field, the magnetization of **7** increases slightly from 0 at 0 T to $0.1N\beta$ at 5 T, because of the predominant population of the ground state $^7F_0$ at 2 K. The difference $\Delta(H) = M_{Cu2Eu2}(H) - M_{Ni2Eu2}(H)$ is slightly higher than the sum of the Brillouin functions for two independent Cu^{II} ions, $2B_{1/2}(H)$, calculated with $S = {}^1/_2$ and $g = 2.00$, shown as the solid line in Figure 4. The result of the field-dependent magnetization thus confirms that there is a small ferromagnetic interaction or no significant magnetic interaction between Cu^{II} and Eu^{III} ions.

(15) Andruh, M.; Bakalbassis, E.; Kahn, O.; Trombe, J.-C.; Porcher, P. *Inorg. Chem.* **1993**, *32*, 1616−1622.

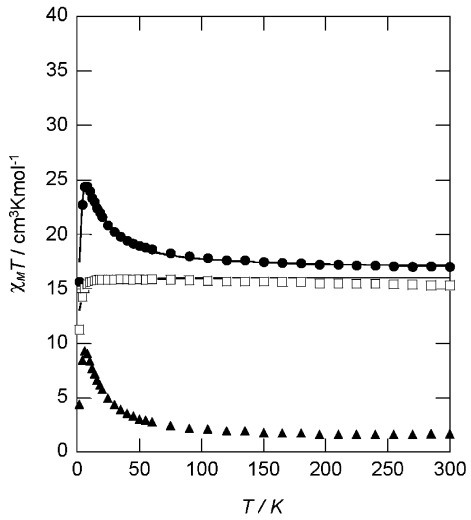

Figure 5. Plots of $\chi_M T$ vs temperature for $[CuLGd(hfac)_2]_2$ (**4**) (●), $[NiLGd(hfac)_2]_2$ (**8**) (□), and the difference $\Delta(T) = (\chi_M T)_{Cu2Gd2} - (\chi_M T)_{Ni2Gd2}$ (▲). The solid line for **4** represents the theoretical curve derived from eqs 7−9 with the parameters $g = 2.02$, $J_1 = +3.1$ cm^{-1}, $J_2 = +1.2$ cm^{-1}, and $zJ' = -0.03$ cm^{-1}. The solid line for **8** represents the theoretical curve derived from eqs 7−9 with the parameters $g = 2.02$ and $zJ' = -0.03$ cm^{-1}.

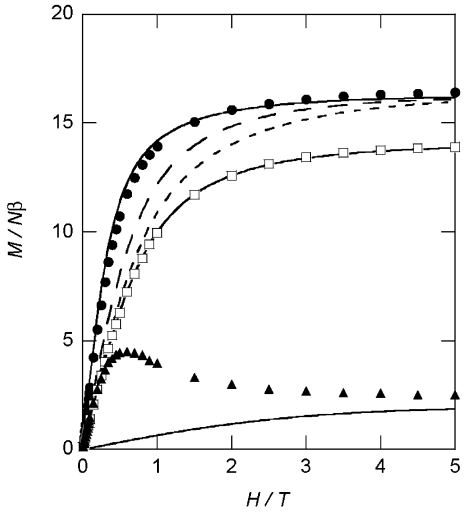

Figure 6. Field dependence of the magnetization of $[CuLGd(hfac)_2]_2$ (**4**) (●), $[NiLGd(hfac)_2]_2$ (**8**) (□), and the difference $\Delta(H) = M_{Cu2Gd2}(H) - M_{Ni2Gd2}(H)$ (▲) at 2 K. The solid lines for **4** and **8** represent the theoretical curves for $g = 2.02$ and $S = 8$ spin state produced by ferromagnetic coupling of the spin system ($^1/_2$, $^7/_2$, $^1/_2$, $^7/_2$) and for two $S = ^7/_2$ and $g = 2.00$ spin states, respectively. The dotted and broken lines represent the theoretical curves for two isolated $S = 4$ spin states and for an isolated spin state of ($^1/_2$, $^7/_2$, $^1/_2$, $^7/_2$). The solid line at the bottom represents the theoretical curve for the sum of the Brillouin functions for two Cu^{II} ions with $S = ^1/_2$ and $g = 2.00$.

Magnetic Properties of $[CuLGd(hfac)_2]_2$ (4) and $[NiLGd(hfac)_2]_2$ (8). The magnetic behavior of **4** and **8** is shown as $\chi_M T$ versus T plots in Figure 5. The $\chi_M T$ value of **4** is 17.06 cm^3 K mol^{-1} at 300 K, this value being slightly larger than the calculated value of 16.51 cm^3 K mol^{-1} expected for two Cu^{II} ($S = ^1/_2$) and two Gd^{III} ($4f^7$, $J = 7/2$, $L = 0$, $S = ^7/_2$, $^8S_{7/2}$) noninteracting ions. The calculated value is derived from eqs 1 and 2 for the case where only one level, $^{2S+1}L_J$, is thermally populated. The ground state of the Gd^{III} ion is $^8S_{7/2}$ with $J = ^7/_2$, $L = 0$, and $S = ^7/_2$, indicating that there is no contribution from orbital angular momentum. Therefore, **4** and **8** can be described as magnetically isotropic molecules. The $\chi_M T$ value of 15.33 cm^3 K mol^{-1} for **8** is almost constant over the whole temperature range except for a decrease in the lowest temperature region, and the reciprocal magnetic susceptibilities follow the Curie law with $C = 15.41$ cm^3 K mol^{-1} in $1/\chi_M = T/C$. The constant value of 15.33 cm^3 K mol^{-1} and the Curie constant of 15.41 cm^3 K mol^{-1} are consistent with the spin-only value of 15.76 cm^3 K mol^{-1} expected for two magnetically isolated Gd^{III} ($S = ^7/_2$) ions, indicating that the Ni^{II} ion is diamagnetic and intra- and intermolecular $Gd^{III}-Gd^{III}$ magnetic interactions are negligibly weak.

On lowering the temperature, the $\chi_M T$ value of **4** increases gradually to reach a maximum value of 24.45 cm^3 K mol^{-1} at 8.0 K and then decreases abruptly. The increase in the higher temperature region indicates the operation of a ferromagnetic interaction between Cu^{II} and Gd^{III} ions. The maximum value of $\chi_M T$ is larger than the calculated value, 20.00 cm^3 K mol^{-1}, expected for two isolated $S = 4$ spins resulting from ferromagnetic coupling between the Cu^{II} ($S = ^1/_2$) and Gd^{III} ($S = ^7/_2$) ions of the dinuclear complex, although the value is smaller than the calculated value, 35.99 cm^3 K mol^{-1}, expected for the $S = 8$ spin of the ferromagnetically coupled $Cu^{II}_2Gd^{III}_2$ system. The abrupt decrease in $\chi_M T$ in the lower temperature region can be ascribed to a weak intra- and/or intermolecular antiferromagnetic interaction.

Comparison of the magnetic properties of **4** with those of **8** give definitive evidence of intramolecular magnetic interaction between Cu^{II} and Gd^{III} ions. The difference $\Delta(T) = (\chi_M T)_{Cu2Gd2} - (\chi_M T)_{Ni2Gd2}$ is plotted in Figure 5. On lowering the temperature, $\Delta(T)$ is almost constant around 1.73 cm^3 K mol^{-1} in the temperature range 300−100 K, increases below 100 K, reaches a maximum of 9.29 cm^3 K mol^{-1} at 6 K, and finally decreases. The positive value and the increase of $J_{CuGd}(T)$ evaluated by this procedure clearly indicate a ferromagnetic interaction between Cu^{II} and Gd^{III} ions.

To reproduce the magnetic susceptibility data of $[CuLGd(hfac)_2]_2$ (**4**) and to evaluate the magnetic interaction parameters, we used the following spin-only Hamiltonian (eq 7), because the Gd^{III} ion assumes an isotropic $^8S_{7/2}$ state without orbital angular momentum:

$$\mathrm{H} = g\beta(S_1 + S_3)\cdot H + g\beta(S_2 + S_4)\cdot H + 2J_1(S_1\cdot S_2 + S_3\cdot S_4) + 2J_2(S_2\cdot S_3 + S_4\cdot S_1) \quad (7)$$

in which H is the applied field and J_1 and J_2 are the Heisenberg coupling constants for the two different magnetic paths shown in Scheme 1, a common g-factor for the Gd^{III} and Cu^{II} ions was used, and the intramolecular $Cu^{II}-Cu^{II}$ and $Gd^{III}-Gd^{III}$ magnetic interactions were neglected on the basis of the results already described. The magnetic susceptibility at each temperature was calculated using the following theoretical eq 8.

$$\chi = M/H = [N\Sigma_i(-\mathrm{d}E_i/\mathrm{d}H)\exp(-E_i/kT)]/[H\Sigma_i\exp(-E_i/kT)] \quad (8)$$

The energy levels of the tetramer, E_i, were evaluated by diagonalizing the Hamiltonian matrix (with dimensions 256×256) in the uncoupled spin function basis set. Moreover, a molecular field term $-zJ'\langle S_z\rangle S_z$ was added to the Hamiltonian to describe the molecular interactions between the tetrameric units. Although small, these interactions are necessary to reproduce the decrease of the magnetic moment below 4 K. The final expression for the magnetic susceptibility becomes

$$\chi_{mf} = \chi/[1 - zJ'\chi/Ng^2\beta^2] \quad (9)$$

where χ is the magnetic susceptibility for the isolated tetramer, calculated as already described. To avoid overparametrization, we fixed g to the value obtained from the fitting of the magnetization data with the Brillouin function for $S = 8$, $g = 2.02$, see later. The magnetic susceptibility data over the entire range of temperatures were well reproduced (with an agreement factor R as low as 2×10^{-5}) with the following best-fit parameters: $g = 2.02$, $J_1 = +3.1$ cm^{-1}, $J_2 = +1.2$ cm^{-1} and $zJ' = -0.03$ cm^{-1}, see solid line in Figure 5. The plus signs of J_1 and J_2 indicate that ferromagnetic interactions are operating between Cu^{II} and Gd^{III} ions both through the amido bridge and the di-μ-oxo bridge. The magnitudes of the J_1 and J_2 values are in the range for previously reported Cu^{II}Gd^{III} polynuclear complexes with an oxo-bridge.[7] As given in the solid line, the magnetic susceptibility of **8** was reproduced by assuming two magnetically isolated Gd^{III} ions with $g = 2.02$ and a small antiferromagnetic intermolecular interaction parameter of -0.03 cm^{-1}. Such a value is exactly the same obtained from the fitting of the magnetic susceptibility data of **4**, and this supports the presence of small intercluster antiferromagnetic interactions in these systems and thus the use of a molecular field term in the spin Hamiltonian (eq 7).

To determine the magnetic interaction and spin ground state, the field dependence of the magnetization was measured up to 5 T at 2 K. Figure 6 shows the field dependence of the magnetization up to 5 T at 2 K for **4** and **8**, with plots of the experimental values of $M/N\beta$ versus H. The empirical approach for the magnetization also gives information on the magnetic interaction between Cu^{II} and Gd^{III} ions. The difference between the magnetization of **4** and **8**, $\Delta(H) = M_{Cu2Gd2}(H) - M_{Ni2Gd2}(H)$, is plotted in Figure 6 and compared with the sum of the Brillouin functions for two independent Cu^{II} ions, $2B_{1/2}(H)$, calculated for $g = 2.00$, the lowest solid curve. We see that $\Delta(H)$ lies well above $2B_{1/2}(H)$ in the whole range of H, thus confirming the ferromagnetic nature of the interaction between Cu^{II} and Gd^{III} ions. The experimental magnetization of **8** is well reproduced by the theoretical curve (solid line) for the sum of the Brillouin functions of two isolated Gd^{III} ($S = {}^7/_2$) ions and $g = 2.00$, demonstrating that the Ni^{II} ion is diamagnetic and the intra- and intermolecular Gd^{III}−Gd^{III} magnetic interaction is negligible. Figure 6 also shows the theoretical curves for the sum of the Brillouin functions of two Cu^{II} ($S = {}^1/_2$) and two Gd^{III} ($S = {}^7/_2$) isolated ions as a broken line, for the sum of two $S = 4$ spins as a dotted line, and for an $S = 8$ spin derived from the ferromagnetic coupling of the spin system ($^1/_2$, $^7/_2$, $^1/_2$, $^7/_2$) as a solid line, respectively. The magnetization data of **4** are larger than those for two independent $S = 4$ spins and for a magnetically isolated ($^1/_2$, $^7/_2$, $^1/_2$, $^7/_2$) system but are well reproduced by the Brillouin function with $S = 8$ and $g = 2.02$ (the upper solid line). Therefore, the curve fitting of the magnetization as well as that of the magnetic susceptibility clearly show that compound **4** has an $S = 8$ spin ground state resulting from the Cu^{II}−Gd^{III} ferromagnetic coupling within the cyclic Cu$^{II}_2$Gd$^{III}_2$ tetramer.

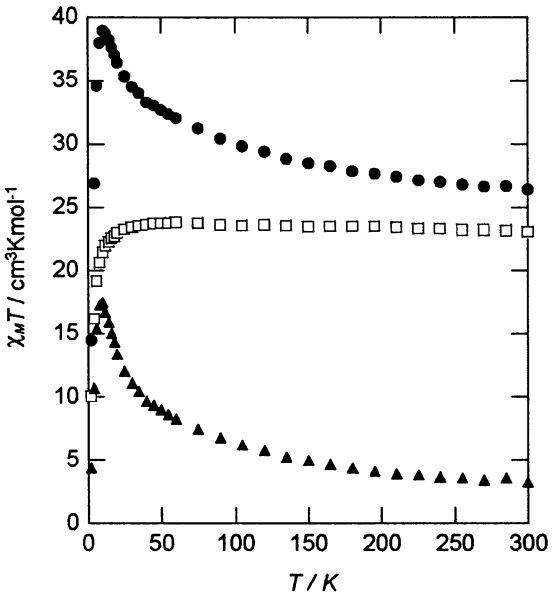

Figure 7. Plots of $\chi_M T$ vs temperature for [CuLTb(hfac)$_2$]$_2$ (**5**) (●), [NiLTb(hfac)$_2$]$_2$ (**9**) (□), and the difference $\Delta(T) = (\chi_M T)_{Cu2Tb2} - (\chi_M T)_{Ni2Tb2}$ (▲).

Magnetic Properties of [CuLTb(hfac)$_2$]$_2$ (5) and [NiLTb(hfac)$_2$]$_2$ (9). The magnetic behavior of **5** and **9** is shown in Figure 7, as plots of $\chi_M T$ versus T. The $\chi_M T$ value of 23.12 cm^3 K mol^{-1} for **9** is almost constant over the whole temperature range except for a decrease in the lowest temperature region, probably due to crystal field effects,[16] and the reciprocal magnetic susceptibility follows the Curie equation of $1/\chi_M = T/C$ with $C = 23.33$ cm^3 K mol^{-1}. The constant value of 23.12 cm^3 K mol^{-1} and the Curie constant of $C = 23.33$ cm^3 K mol^{-1} are consistent with the value 23.64 cm^3 K mol^{-1} expected for two independent Tb^{III} (4f^8, $J = 6$, $S = 3$, $L = 3$, $^7F_6$) ions and two diamagnetic Ni^{II} ions, indicating that the magnetic moment of the Tb^{III} ion is well reproduced by eq 2. The $\chi_M T$ value at 300 K of **5** is 26.42 cm^3 K mol^{-1}. The reciprocal magnetic susceptibilities in the temperature range of 50−300 K follow the Curie−Weiss equation of $1/\chi_M = (T - \theta)/C$ with the Curie constant of 25.42 cm^3 K mol^{-1} and the Weiss constant of +14.3 K. The Curie constant is compatible with the calculated value 24.39 cm^3 K mol^{-1} expected for two Cu^{II} ($S = {}^1/_2$) and two Tb^{III} (4f^8, $J = 6$, $S = 3$, $L = 3$, $^7F_6$) magnetically isolated ions. On lowering the temperature, the $\chi_M T$ value of **5** increases gradually to reach a maximum value of 38.97 cm^3

(16) Casey, A. T.; Mitra, S. In *Theory and Applications of Molecular Paramagnetism*; Boudreaux, E. A., Mulay L. N., Eds.; Interscience: New York, 1976; pp 135 and 271.

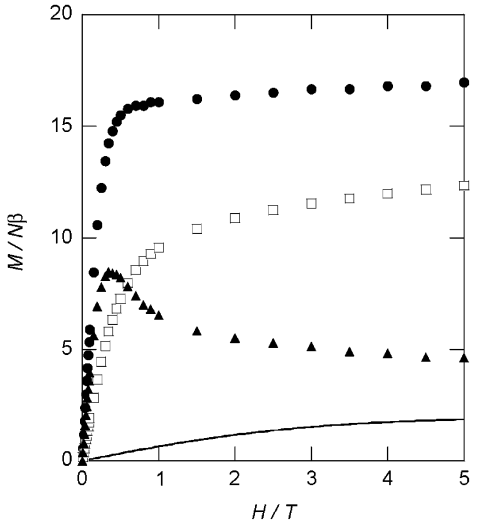

Figure 8. Field dependence of the magnetization of $[CuLTb(hfac)_2]_2$ (**5**) (●), $[NiLTb(hfac)_2]_2$ (**9**) (□), and the difference $\Delta(H) = M_{Cu2Tb2}(H) - M_{Ni2Tb2}(H)$ (▲) at 2 K. The solid line represents the theoretical curve for the sum of the Brillouin functions for two Cu^{II} ions with $S = {}^1/_2$ and $g = 2.00$.

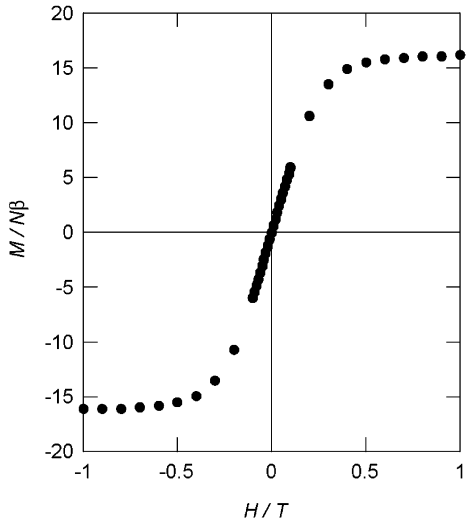

Figure 9. Magnetization loop of $[CuLTb(hfac)_2]_2$ (**5**) at 2 K in the sequence from 0 T → +1 T → −1 T → 0 T.

K mol^{-1} at 10 K and then decreases abruptly. The increase in the higher temperature region and the positive Weiss constant indicate the operation of a ferromagnetic interaction between the Cu^{II} and Tb^{III} ions.

Comparison of the magnetic susceptibilities of **5** with those of **9** gives more reliable information on the intramolecular magnetic interaction between Cu^{II} and Tb^{III} ions. The difference $\Delta(T) = (\chi_M T)_{Cu2Tb2} - (\chi_M T)_{Ni2Tb2}$ is plotted and inserted in Figure 7. On lowering the temperature, $\Delta(T)$ increases gradually from 3.57 cm^3 K mol^{-1} at 300 K, reaches a maximum of 17.50 cm^3 K mol^{-1} at 10 K, and finally decreases abruptly to 4.41 cm^3 K mol^{-1} at 2 K, still above the value of 0.75 cm^3 K mol^{-1} for two noninteracting Cu^{II} ions. The pronounced positive deviation of $J_{CuTb}(T)$ clearly indicates a ferromagnetic interaction between Cu^{II} and Tb^{III} ions.

Figure 8 shows the field dependence of the magnetization up to 5 T at 2 K for **5** and **9**, with plots of the experimental values of $M/N\beta$ versus H. On increasing the applied external magnetic field, the magnetization of **9** increases to 12.3 $N\beta$ at 5 T but does not reach the expected saturation value of 18 $N\beta$ (9 $N\beta$ for each Tb^{III} ion). This is due to a crystal field effect on the Tb^{III} ion that removes the 13-fold degeneracy of the $^7F_6$ ground state.[16] The highest of the levels into which the $^7F_6$ state is split do not contribute to the magnetization, which therefore does not reach the saturation value. This effect is well-known for transition metal ions with a significant zero field splitting and also applies to rare earth ions except for Gd^{III} ion with its isotropic ground $^8S_{7/2}$ state. The difference $\Delta(H) = M_{Cu2Tb2}(H) - M_{Ni2Tb2}(H)$ is plotted in Figure 8 and compared with the sum of the Brillouin functions for two independent Cu^{II} ions, $2B_{1/2}(H)$, calculated for $g = 2.00$. We see that $\Delta(H)$ lies well above $2B_{1/2}(H)$ in the whole range of H, thus confirming the ferromagnetic nature of the interaction between Cu^{II} and Tb^{III} ions. The magnetization loop of **5** was measured at 2 K in the −1 T to +1 T magnetic field range, and the result is shown in Figure 9. No hysteresis was observed at 2 K under the experimental condition.

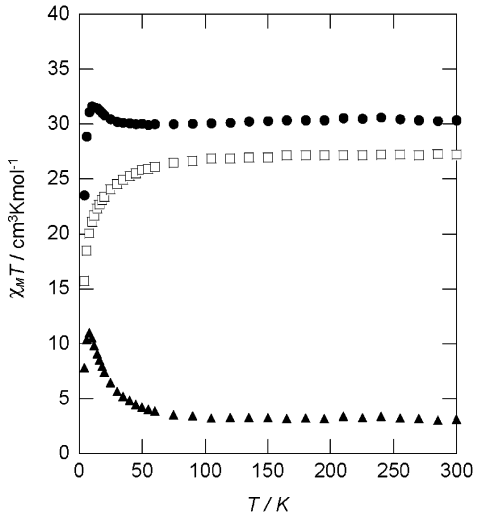

Figure 10. Plots of $\chi_M T$ vs temperature for $[CuLDy(hfac)_2]_2$ (**6**) (●), $[NiLDy(hfac)_2]_2$ (**10**) (□), and the difference $\Delta(T) = (\chi_M T)_{Cu2Dy2} - (\chi_M T)_{Ni2Dy2}$ (▲).

Magnetic Properties of $[CuLDy(hfac)_2]_2$ (6) and $[NiLDy(hfac)_2]_2$ (10). The magnetic behavior of **6** and **10** is shown in Figure 10, as $\chi_M T$ versus T. The $\chi_M T$ value of 27.24 cm^3 K mol^{-1} for **10** is almost constant over the temperature range 300−150 K and then decreases gradually in the lower temperature region because of crystal field effects. The reciprocal magnetic susceptibility follows the Curie law with $C = 27.59$ cm^3 K mol^{-1} in the equation $1/\chi_M = T/C$. The constant value of 27.24 cm^3 K mol^{-1} and the Curie constant of $C = 27.59$ cm^3 K mol^{-1} are compatible with the value of 28.34 cm^3 K mol^{-1} expected for two magnetically isolated Dy^{III} ($4f^9$, $J = {}^{15}/_2$, $S = {}^5/_2$, $L = 5$, $^6H_{15/2}$) ions and two diamagnetic Ni^{II} ions. The $\chi_M T$ value at 300 K of **6** is 30.38 cm^3 K mol^{-1}, a value that is compatible with the calculated value of 29.09 cm^3 K mol^{-1} expected for two Cu^{II} ($S = {}^1/_2$) and two Dy^{III} ($4f^9$, $J = {}^{15}/_2$, $S = {}^5/_2$, $L = 5$, $^6H_{15/2}$)

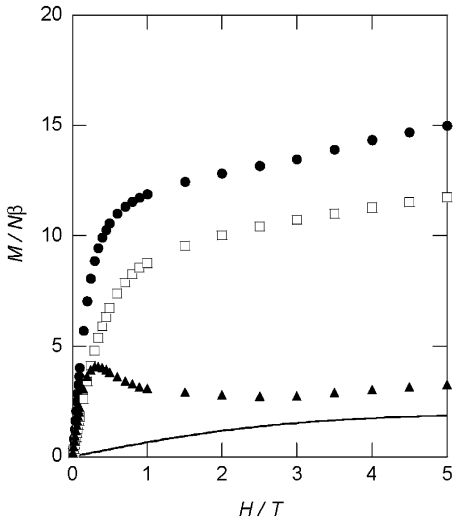

Figure 11. Field dependence of the magnetization of $[CuLDy(hfac)_2]_2$ (**6**) (●), $[NiLDy(hfac)_2]_2$ (**10**) (□), and the difference $\Delta(H) = M_{Cu2Dy2}(H) - M_{Ni2Dy2}(H)$ (▲) at 2 K. The solid line represents the theoretical curve for the sum of the Brillouin functions for two Cu^{II} ions with $S = {}^1/_2$ and $g = 2.00$.

magnetically isolated ions. On lowering the temperature, the $\chi_M T$ value of **6** is almost constant from 300 to 20 K, and then, it slightly increases to reach a maximum value of 31.62 cm^3 K mol^{-1} at 10 K and finally decreases abruptly. The difference $\Delta(T) = (\chi_M T)_{Cu2Dy2} - (\chi_M T)_{Ni2Dy2}$ is plotted and inserted in Figure 10. On lowering the temperature, $\Delta(T)$ increases gradually from 3.14 cm^3 K mol^{-1} at 300 K, reaches a maximum at 8 K, and finally decreases to 7.82 cm^3 K mol^{-1} at 4 K, still above the value of 0.75 cm^3 K mol^{-1} for two noninteracting Cu^{II} ions. The pronounced positive value of J_{CuDy} indicates a ferromagnetic interaction between Cu^{II} and Dy^{III} ions.

Figure 11 shows the field dependence of the magnetization up to 5 T at 2 K for **6** and **10**, with plots of the experimental values of $M/N\beta$ versus H. On increasing the applied external magnetic field, the magnetization of **10** increases to 11.7 $N\beta$ at 5 T but does not reach the expected saturation value of 20 $N\beta$(10 $N\beta$ per each Dy^{III} ion). This is again due to crystal field effects on the Dy^{III} ion, which remove the 16-fold degeneracy of the $^6H_{15/2}$ ground state.[17] The difference $\Delta(H) = M_{Cu2Dy2}(H) - M_{Ni2Dy2}(H)$ is plotted in Figure 11, together with the sum of the Brillouin functions for two independent Cu^{II} ions, $2B_{1/2}(H)$, calculated for $g = 2.00$. We see that $\Delta(H)$ lies well above $2B_{1/2}(H)$ in the whole range of H, thus confirming the ferromagnetic nature of the interaction between Cu^{II} and Dy^{III} ions.

Molecular Magnetic Anisotropy? We suggested the presence of a large magnetic anisotropy in our tetrameric clusters except for the Cu_2Gd_2 cluster, mainly for the most interesting Cu_2Tb_2 and Cu_2Dy_2 clusters, only on the basis of the nonsaturation of the magnetization versus H curves for the Ni_2Tb_2 and Ni_2Dy_2 clusters to the values expected for two isolated isotropic Tb^{III} ($g = {}^3/_2$, $J = 6$) and Dy^{III} ($g = {}^4/_3$, $J = {}^{15}/_2$) ions, respectively. These curves confirm the single-ion anisotropy of these Tb^{III} and Dy^{III} ions, which is well-known for rare earth ions. We can reasonably expect that this single-ion anisotropy leads to the molecular anisotropy of Cu_2Tb_2 and Cu_2Dy_2 clusters. However, it is in principle difficult to characterize quantitatively the ground state and the molecular anisotropy of the Cu_2Tb_2 and Cu_2Dy_2 clusters not only from theoretical but also experimental viewpoints. In principle, we have enough data for a fitting of the magnetization of Cu_2Tb_2 and Cu_2Dy_2 clusters as a function of H. However, there has been no reported theory on the coupling of two or more lanthanide ions with first-order angular momentum. Not only can no simple interaction parameters (like the coupling constant J for transition metal clusters) be defined, but also no good quantum number (such as spin or total quantum number S and J) can characterize the ground and excited states of the d−f cluster. Actually, S is a good quantum number only for the Gd^{III} ions with zero angular momentum, and we have seen discussion of the ground state of transition metal−lanthanide clusters only for Gd^{III}. For other lanthanide compounds, J may be a good quantum number, but for a cluster with both lanthanide and transition metal ions.

Concluding Remarks. Four pairs of cyclic cylindrical tetranuclear complexes $[CuLLn(hfac)_2]_2$ and $[NiLLn(hfac)_2]_2$ with $4f^{6-9}$ electronic configurations of the Ln^{III} ions (Ln^{III} = Eu^{III}, Gd^{III}, Tb^{III}, and Dy^{III}) were synthesized, and the magnetic properties were investigated by their temperature-dependent magnetic susceptibility and field-dependent magnetization. Comparison of the magnetic properties of a $Cu^{II}_2Ln^{III}_2$ complex with those of the corresponding $Ni^{II}_2Ln^{III}_2$ complex showed that the magnetic interaction between Cu^{II} and Eu^{III} ions is weakly ferromagnetic or negligibly small and that between Cu^{II} and either of the Gd^{III}, Tb^{III}, and Dy^{III} ions is ferromagnetic. The ferromagnetic nature of the interaction between Cu^{II} and either of the Gd^{III}, Tb^{III}, and Dy^{III} ions for the present cyclic tetranuclear complexes is consistent with the ferromagnetic nature of dinuclear $Cu^{II}Ln^{III}$ compounds reported by Costes et al.,[13] and 2D ladder-type $Ln^{III}_2Cu^{II}_3$ compounds reported by Kahn et al.[14] The magnetization measurements for a pair of $Cu^{II}_2Ln^{III}_2$ and $Ni^{II}_2Ln^{III}_2$ are very effective in revealing not only the nature of the Cu^{II}−Ln^{III} magnetic interaction but also the magnetic anisotropy. This study has demonstrated that the 3d−4f cyclic cylindrical structure is a suitable molecular design to generate a large magnetic moment and large magnetic anisotropy, possibly leading to a single molecule magnet. It is in principle difficult to characterize quantitatively the ground state and the molecular anisotropy for a cluster with both lanthanide and transition metal ions, because there has been no theory on the magnetic properties for a cluster with both lanthanide and transition metal ions. Synthetic efforts and magnetic measurements based on the d−f clusters may lead to the single molecule magnet.

Experimental Section

Materials. All chemicals and solvents used for the synthesis were reagent grade and were obtained from Tokyo Kasei Co. Ltd. and used without further purification.

(17) Richardson, M. F.; Wagner, W. F.; Sands, D. E. *J. Inorg. Nucl. Chem.* **1968**, *30*, 1275−1289.

1-(2-Hydroxybenzamido)-2-(2-hydroxy-3-methoxybenzylideneamino)ethane (H_3L). Ethyl salicylate (16.627 g, 0.1 mol) and ethylenediamine (6.037 g, 0.1 mol) were mixed, and the mixture was refluxed for 5 h at 110 °C. The mixture was cooled to room temperature, and 50 mL of methanol was added. After the solution was allowed to stand for 1 day, it was evaporated to dryness. Acetone (50 mL) was added to the reaction product and allowed to stand for several hours. Meanwhile, an intermediate product was obtained. The intermediate product (4.413 g, 20 mmol) and 3-methoxysalicylaldehyde (3.043 g, 20 mmol) were stirred in ethanol for 1 h with heating. The reaction product was recrystallized from ethanol, producing yellow needles. Yield: 3.604 g (57%). IR (cm^{-1}): $\nu_{C=O}$ 1649; $\nu_{C=N}$ 1634. Anal. Calcd for $C_{17}H_{18}N_2O_4$: C 64.96, H 5.77, N 8.91. Found: C 64.85, H 5.80, N 8.89%.

K[CuL] (1). Copper(II) acetate monohydrate (0.602 g, 3 mmol) and H_3L (0.948 g, 3 mmol) were dissolved in methanol (60 mL). Potassium *t*-butoxide (1.011 g, 9 mmol) was added to the resulting solution, and the mixture was stirred for 2 h with heating and then filtered to give a violet powder. Yield: 0.914 g (74%). IR (cm^{-1}): $\nu_{C=O}$ 1644; $\nu_{C=N}$ 1600. Anal. Calcd for $C_{17}H_{15}KCuN_2O_4$: C 49.32, H 3.65, N 6.77. Found: C 49.28, H 3.66, N 6.72%.

K[NiL]·2.5H_2O (2). Nickel(II) acetate tetrahydrate (0.749 g, 3 mmol) and H_3L (0.947 g, 3 mmol) were dissolved in methanol (50 mL). Potassium *t*-butoxide (1.014 g, 9 mmol) was added to the resulting solution, and the mixture was stirred for 1 h and filtered to give an orange powder. Yield: 0.625 g (51%). IR (cm^{-1}): $\nu_{C=O}$ 1625; $\nu_{C=N}$ 1600. Anal. Calcd for $C_{17}H_{20}KNiN_2O_{6.5}$: C 44.96, H 4.44, N 6.17. Found: C 44.95, H 3.93, N 6.18%.

[Ln(hfac)$_3$(H_2O)$_2$]. These lanthanide(III) complexes were prepared by mixing $Ln(OAc)_3 \cdot nH_2O$ and hexafluoroacetylacetone in 1:3 mol ratio in water according to the literature.[17]

[CuLEu(hfac)$_2$]$_2$ (3). A methanolic solution (20 mL) of **1** (0.104 g, 0.25 mmol) was gently poured into a methanolic solution (20 mL) of Eu(hfac)$_3$(H_2O)$_2$ (0.203 g, 0.25 mmol) at ambient temperature. The resulting solution was allowed to stand for several days. The solution became almost colorless, and the dark reddish purple crystals that formed were collected by filtration and dried in air. The crystals were sparingly soluble even in *N*,*N*-dimethylformamide (DMF), and recrystallization was not performed. Dark reddish purple crystals were obtained. Yield: 0.208 g (88%). IR (cm^{-1}): $\nu_{C=O}$ 1651; $\nu_{C=N}$ 1603; ν_{CF} 1255−1143. Anal. Calcd for $C_{54}H_{34}Cu_2Eu_2N_4O_{16}F_{24}$: C 34.47, H 1.82, N 2.98. Found: C 34.52, H 1.85, N 2.98%.

[CuLGd(hfac)$_2$]$_2$ (4). This complex was prepared by the same method as for **3**, using Gd(hfac)$_3$(H_2O)$_2$ instead of Eu(hfac)$_3$(H_2O)$_2$. Dark reddish purple crystals were obtained. Yield: 0.205 g (87%). IR (cm^{-1}): $\nu_{C=O}$ 1652; $\nu_{C=N}$ 1604; ν_{CF} 1255−1144. Anal. Calcd for $C_{54}H_{34}Cu_2Gd_2N_4O_{16}F_{24}$: C 34.27, H 1.81, N 2.96. Found: C 34.37, H 1.85, N 2.95%.

[CuLTb(hfac)$_2$]$_2$ (5). This complex was prepared by the same method as for **3**, using Tb(hfac)$_3$(H_2O)$_2$ instead of Eu(hfac)$_3$(H_2O)$_2$. Dark reddish purple crystals were obtained. Yield: 0.203 g (86%). IR (cm^{-1}): $\nu_{C=O}$ 1651; $\nu_{C=N}$ 1604; ν_{CF} 1252−1149. Anal. Calcd for $C_{54}H_{34}Cu_2Tb_2N_4O_{16}F_{24}$: C 34.21, H 1.81, N 2.96. Found: C 34.36, H 1.88, N 2.92%.

[CuLDy(hfac)$_2$]$_2$ (6). This complex was prepared by the same method as for **3**, using Dy(hfac)$_3$(H_2O)$_2$ instead of Eu(hfac)$_3$(H_2O)$_2$. Dark reddish purple crystals were obtained. Yield: 0.197 g (83%). IR (cm^{-1}): $\nu_{C=O}$ 1653; $\nu_{C=N}$ 1604; ν_{CF} 1255−1144. Anal. Calcd for $C_{54}H_{34}Cu_2Dy_2N_4O_{16}F_{24}$: C 34.08, H 1.80, N 2.94. Found: C 34.46, H 1.88, N 3.07%.

[NiLEu(hfac)$_2$]$_2$ (7). This complex was prepared by the same method as for **3**. Orange microcrystals were obtained. Yield: 0.195 g (85%). IR (cm^{-1}): $\nu_{C=O}$ 1652; $\nu_{C=N}$ 1602; ν_{CF} 1255−1145. Anal. Calcd for $C_{54}H_{34}Ni_2Eu_2N_4O_{16}F_{24}$: C 34.64, H 1.83, N 2.99. Found: C 34.87, H 1.79, N 3.18%.

[NiLGd(hfac)$_2$]$_2$ (8). This complex was prepared by the same method as for **7**, using Gd(hfac)$_3$(H_2O)$_2$ instead of Eu(hfac)$_3$(H_2O)$_2$. Orange microcrystals. Yield: 0.198 g (84%). IR (cm^{-1}): $\nu_{C=O}$ 1652; $\nu_{C=N}$ 1602; ν_{CF} 1254−1145. Anal. Calcd for $C_{54}H_{34}Ni_2Gd_2N_4O_{16}F_{24}$: C 34.45, H 1.82, N 2.98. Found: C 34.66, H 1.82, N 3.11%.

[NiLTb(hfac)$_2$]$_2$ (9). This complex was prepared by the same method as for **7**, using Tb(hfac)$_3$(H_2O)$_2$ instead of Eu(hfac)$_3$(H_2O)$_2$. Orange microcrystals were obtained. Yield: 0.194 g (83%). IR (cm^{-1}): $\nu_{C=O}$ 1652; $\nu_{C=N}$ 1602; ν_{CF} 1255−1145. Anal. Calcd for $C_{54}H_{34}Ni_2Tb_2N_4O_{16}F_{24}$: C 34.39, H 1.82, N 2.97. Found: C 34.62, H 1.80, N 3.11%.

[NiLDy(hfac)$_2$]$_2$ (10). This complex was prepared by the same method as for **7**, using Dy(hfac)$_3$(H_2O)$_2$ instead of Eu(hfac)$_3$(H_2O)$_2$. Orange microcrystals were obtained. Yield: 0.194 g (83%). IR (cm^{-1}): $\nu_{C=O}$ 1653; $\nu_{C=N}$ 1602; ν_{CF} 1256−1145. Anal. Calcd for $C_{54}H_{34}Ni_2Dy_2N_4O_{16}F_{24}$: C 34.26, H 1.81, N 2.96. Found: C 34.28, H 1.89, N 3.13%.

Physical Measurements. Elemental C, H, and N analyses were carried out at the Elemental Analysis Service Center of Kyushyu University and at the Center for Instrumental Analysis of Kumamoto University. Infrared spectra were recorded on a Perkin Elmer FT-IR spectrometer PARAGON 1000 using KBr disks. X-ray powder diffraction patterns were measured by a Rigaku X-ray diffractometer RAD-2A with Cu Kα radiation at room temperature. FAB mass spectra were recorded in *N*,*N*-dimethylformamide as solvent and 3-nitrobenzyl alcohol matrix with a JEOL JMS600. Temperature-dependent magnetic susceptibilities in the temperature range 2−300 K under a constant external magnetic field of 1 T and field-dependent magnetization measurements in an applied magnetic field from 0 to 5 T at 2 K were measured with an MPMS5 SQUID susceptometer (Quantum Design, Inc.). The calibrations were performed with palladium. Corrections for diamagnetism were applied using Pascal's constants.[1]

X-ray Data Collection, Reduction, and Structure Determination. X-ray data were collected on a Rigaku AFC7R diffractometer with graphite monochromated Mo Kα radiation (λ = 0.71069 Å) and a 12 kW rotating anode generator. The data were collected at a temperature of 20 ± 1 °C using the $\omega-2\theta$ scan technique to a maximum 2θ value of 50.0° at scan speeds of 8.0−16.0°/min (in ω). The weak reflections ($I < 10.0\sigma(I)$) were rescanned (maximum of 5 scans), and the counts were accumulated to ensure good counting statistics. Stationary background counts were recorded on each side of the reflection. The ratio of peak to background counting time was 2:1. The intensities of three representative reflections were measured after every 150 reflections. Over the course of the data collection, the standard reflections were monitored, and decay corrections were applied through a polynomial correction. An empirical absorption correction based on azimuthal scans of several reflections was applied. The data were also corrected for Lorentz and polarization effects. A correction for secondary extinction was applied.[18]

The structures were solved by direct methods[19] and expanded using the Fourier technique.[20] The non-hydrogen atoms were refined

(18) Larson, A. C. *Crystallographic Computing, 291−294*; Ahmed, F. R., Ed.; Munksgaard: Copenhagen, 1970 (eq 22, with *V* replaced by the cell volume).

(19) *DIRDIF99*: Beurskens, P. T.; Admiraal, G.; Beurskens, G.; Bosman, W. P.; de Gelder, R.; Israel, R.; Smits, J. M. M. *The DIRDIF-99 program system*; Technical Report of the Crystallography Laboratory; University of Nijmegen: Nijmegen, The Netherlands, 1999.

anisotropically. Hydrogen atoms at their calculated positions were included in the structure factor calculation but were not refined. Full-matrix least-squares refinement based on the observed reflections ($I > 2.00\sigma(I)$) was employed, where the unweighted and weighted agreement factors of $R = \sum||F_o| - |F_c||/\sum|F_o|$ and $R_w = [\sum w(|F_o| - |F_c|)^2/\sum w|F_o|^2]^{1/2}$ were used. The weighting scheme was based on counting statistics. Plots of $\sum w(|F_o| - |F_c|)^2$ versus $|F_o|$, reflection order in data collection, sin θ/λ, and various classes of indices showed no unusual trends. Neutral atomic scattering factors were taken from Cromer and Waber.[21] Anomalous dispersion effects were included in F_{calcd}; the values $\Delta f'$ and $\Delta f''$ were those of Creagh and McAuley.[22] The values for the mass attenuation coefficients were those of Creagh and Hubbel.[23] All calculations were performed using the CrystalStructure crystallographic software package.[24,25]

Acknowledgment. This work was supported by a Grant-in-Aid for Scientific Research (14340209) from the Ministry of Education, Science, and Culture, Japan. We are grateful to JSPS (Japan Society of Promotion for Science) for the bilateral exchange program.

Supporting Information Available: X-ray crystallographic files in CIF format for compounds **4** and **5**. This material is available free of charge via the Internet at http://pubs.acs.org.

IC026045D

(20) *SIR92*: Altomare, A.; Cascarano, G.; Giacovazzo, C.; Guagliardi, A.; Burla, M.; Polidori, G.; Camalli, M. *J. Appl. Crystallogr.* **1994**, *27*, 435.
(21) Cromer, D. T.; Waber, J. T. In *International Tables for X-ray Crystallography*, Vol. IV; The Kynoch Press: Birmingham, England, 1974; Table 2.2 A.
(22) Creagh, D. C.; McAuley, W. J. In *International Tables for Crystallography*, Vol C; Wilson, A. J. C., Ed.; Kluwer Academic Publishers: Boston, 1992; Table 4.2.6.8, pp 219−222.
(23) Creagh, D. C.; Hubbell, J. H. In *International Tables for Crystallography*, Vol C.; Wilson, A. J. C., Ed.; Kluwer Academic Publishers: Boston, 1992; Table 4.2.4.3, pp 200−206.
(24) *CrystalStructure 2.00*; Crystal Structure Analysis Package, Rigaku and Molecular Structure Corp., 2001.
(25) Watkin, D. J.; Prout, C. K.; Carruthers, J. R.; Betteridge, P. W. *CRYSTALS*, Issue 10; Chemical Crystallography Laboratory: Oxford, U.K.